



Performance assessment of concrete walls reinforced with GFRP bars

Nayera Mohamed¹, Ahmed Farghaly², Murat Saatcioglu³, Brahim Benmohrane⁴

¹ Former Post-Doctoral, Department of Civil Engineering, University of Sherbrooke - Sherbrooke, QC, Canada, Lecturer, Department of Civil Engineering, Assiut University - Assiut, Egypt.

² Research Associate, Department of Civil Engineering, University of Sherbrooke - Sherbrooke, QC, Canada.

³ Professor, Department of Civil Engineering, University of Ottawa - Ottawa, ON, Canada

⁴ Professor, Department of Civil Engineering, University of Sherbrooke - Sherbrooke, QC, Canada.

ABSTRACT

The performance-based assessment and design become more wide-spread in structural engineering practice. The relationship between deformation limits and performance levels (immediate occupancy, life safety, and collapse prevention) are reasonably well established for steel-reinforced concrete (RC) walls. However, performance of RC walls reinforced with fiber-reinforced-polymer (FRP) bars can be substantially different. Four full-scale shear wall specimens were tested; two specimens were reinforced with glass-FRP (GFRP) bars, while the other two specimens were reinforced with steel bars. Analysis of the experimental observation defined the three performance levels and compared to the specified limits provided in the ASCE/SEI 41-06 in the drift ratio format. It was found that, the GFRP-RC shear walls developed significant deformability, exceeding the ASCE/SEI 41-06 deformation performance limits due to the elastic nature of the GFRP bars. This suggested proposing new deformation limits for the GFRP-RC walls associated with the damage description of each of the three performance levels

Keywords: concrete walls, GFRP bars, deformation limit, performance level.

INTRODUCTION

Reinforced concrete (RC) shear walls provide strength, stiffness and energy dissipation capacity to earthquake resistant buildings, forming a preferred lateral force resisting system in buildings [1]. The walls provide drift control, thereby reducing both structural and non-structural damage to buildings during strong earthquakes. They can also be designed to provide sufficient strength and ductility, providing resistance to earthquake forces while dissipating seismic-induced energy. The preferred mode of behavior in structural shear walls is flexural mode. Therefore, the current seismic-resistant design philosophy is based on promoting flexural yielding and preventing brittle shear failure [2,3]. Significant research has been conducted on flexure-dominant steel-RC structural walls. However, research on shear walls reinforced internally with fiber-reinforced-polymer (FRP) bars for new buildings is scarce in the literature. Limited research was conducted by Mohamed et al. [4-6] and provided valuable test data on large scale FRP-RC shear walls under reversed cyclic loading.

As performance-based building assessment and design become more wide-spread in structural engineering practice, the required analytical tools gain importance to quantify shear wall performance levels. In ASCE/SEI 41 [7] four performance levels were defined as operational, immediate occupancy, life safety and collapse prevention, in order of severity in damage. The operational performance level is governed by non-structural damage, but the latter three are specified as “structural performance levels”. They are quantified in terms of drift ratios for overall structural performance limits. Accordingly, immediate occupancy limit for concrete shear walls is specified as 0.5% drift ratio. This level is associated with the damage in structural members is limited to cracking of concrete in the effective elastic range of deformations prior to the yielding of reinforcement. Life safety performance level is specified as 1.0% drift ratio for the walls with Major cracking and some spalling of concrete is expected with reinforcing steel entering into the post-yield range, but the structure remains stable with sufficient strength and deformability to ensure life safety. Collapse prevention corresponds to a maximum story drift ratio of 2.0% for RC shear walls and marks the ultimate limit prior to collapse with possibility of demolishing the building after the earthquake. At this level of deformation, up to 20% of strength decay is usually permissible because of the inherent redundancy in monolithically built multi-story RC buildings [8].

While the relationship between deformation limits and performance levels are reasonably well established for steel-RC walls, performance of FRP-RC walls can be substantially different with experimental data and research lacking for this type of application. FRP reinforcement has lower modulus of elasticity, resulting in softer response upon concrete cracking. Furthermore, FRP re-bars show higher rupturing strength in tension, lower strength in compression and brittle material behavior

with linear stress-strain relationships. These aspects of FRP behavior may raise questions on deformability of FRP-RC shear walls and their suitability as seismic resistant elements. However, as later illustrated in the paper, FRP-RC shear walls develop significant deformability, meeting and overstepping the ASCE/SEI 41 [7] drift performance levels described above.

Although the deformation limits specified in ASCE/SEI 41 [7,9] are given either in the form of drift ratio or plastic rotations (ASCE/SEI 41 [7] and ASCE/SEI 41 [9], respectively) for concrete structural walls, this paper focuses mainly on calibrating the performance and damage levels to assess the GFRP-RC shear walls based on drift ratio. The three performance levels; immediate occupancy, life safety, and collapse prevention, were identified according to the specified definition of each of the damage level in ASCE/SEI 41 [7]. New drift ratios for each performance level was proposed accordingly. The results provide much needed guidance to structural engineers for use of FRP reinforcement in earthquake resistant shear walls.

EXPERIMENTAL PROGRAM

The presented experimental program consists of four full-scale shear walls, representing one-story prototype mid-rise shear walls, tested under quasi-static reversed cyclic loading and a constant axial concentric load of 7% of the wall axial capacity. The walls were cycled twice at each displacement level with increments of 0.06% up to 0.3% lateral drift, followed by increments of 0.15% up to 1.5%, and then increments of 0.3% to failure. A series of linear variable differential transducers (LVDTs) and strain gauges were used to measure critical-response quantities as shown in Figure 1. Reinforcement and geometric details of the test specimens in addition to the instrumentations are presented in Table 1 and Figure 1. The details of test setup, loading procedure, and instrumentation can be found in Mohamed et al. [4].

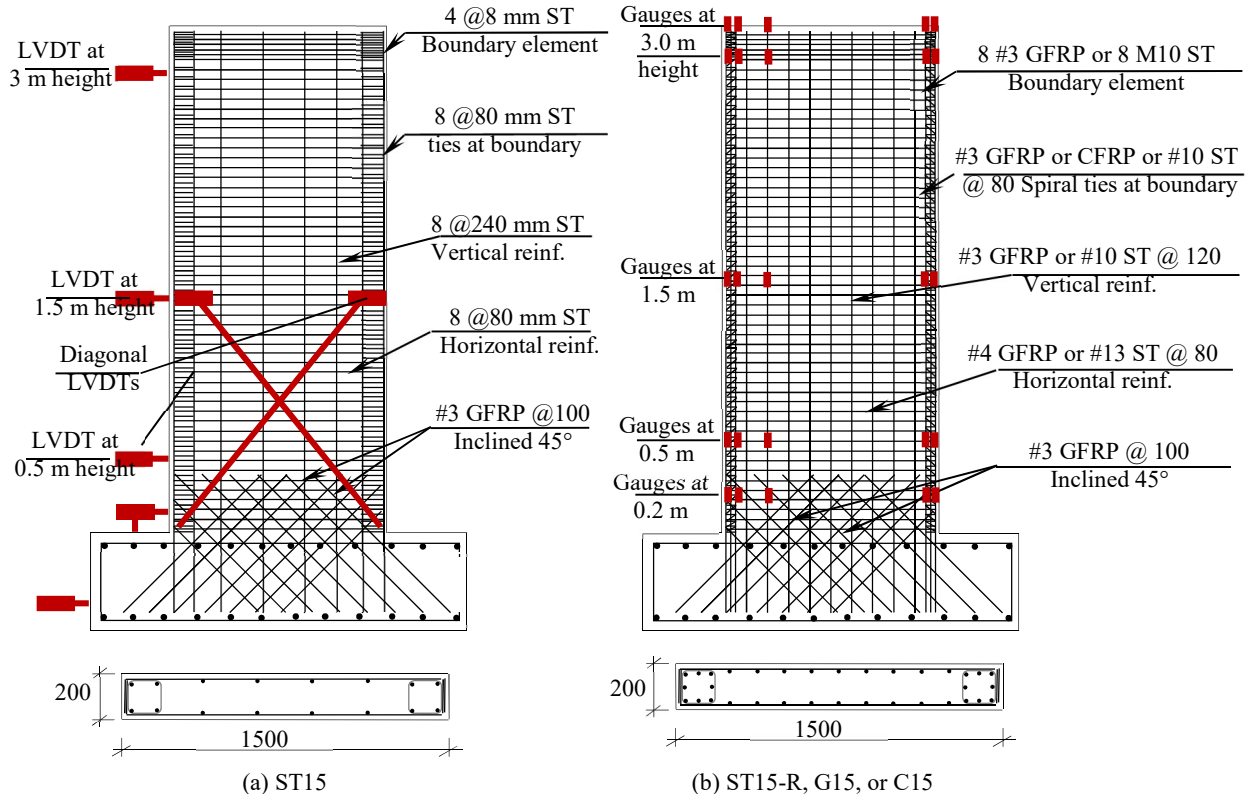


Figure 1. Reinforcement details and concrete dimensions of the tested shear-wall specimens.

The four walls consist of specimens ST15, ST15-R, G15, and C15. The experimental results of specimens ST15 and G15 were reported earlier by Mohamed et al. (2014a), while specimens ST15-R and C15 are newly tested and added to the current performance assessment investigation.

The two new specimens (ST15-R and C15) along with specimens ST15 and G15 represent mid-rise walls with an aspect ratio (height-to-length ratio h_w/l_w) of 2.33. They were 3500 mm high, 1500 mm long, and 200 mm thick. This implies that the walls were subjected to shear, developing sizeable shear distortions, though they were designed to prevent premature shear failure. Two of the walls were reinforced with steel bars and the other two with FRP bars. ST15 was reinforced with deformed 8- mm diameter steel bars to provide the minimum vertical web and boundary element reinforcement ratios specified in ACI 318 [2] and CSA A23.3 [3]. G15 and C15 were designed to have GFRP bars with the same reinforcement axial stiffness ($A_f \times E_f$) as ST15, except for the boundary element transverse reinforcement. G15 had GFRP spiral stirrups in the wall boundary elements,

whereas C15 had equal percentage of CFRP spiral stirrups. ST15-R had steel reinforcement ratio as the reinforcement ratio of G15. The walls' reinforcement ratio is presented in Table 1. Table 2 provides mechanical properties of all the reinforcement used in the experimental program.

Table 1. Wall specimens

Specimen	h_w/l_w	Web RFT		Boundary RFT		Reinforcement ratio				f_c'
		VI bars	H _z bars	VI bars	Spiral stirrups	$\rho_v\%$	$\rho_h\%$	$\rho_l\%$	$\rho_t\%$	
ST15*	2.33	Steel 8 mm	Steel 8 mm	4 Steel 8 mm	Steel 8 mm	0.23	0.63	0.5	0.63	39.2
ST15-R		Steel #3	Steel #4	8 Steel #3	Steel #3	0.58	1.25	1.42	1.6	39.5
G15*		GFRP #3	GFRP #4	8 GFRP #3	GFRP #3	0.58	1.58	1.43	0.89	39.9
C15		GFRP #3	GFRP #4	8 GFRP #3	CFRP #3	0.58	1.58	1.43	0.89	40.1

* reported in Mohamed et al. [4]. h_w/l_w wall aspect ratio; h_w wall height; l_w wall length; ρ_v vertical web-reinforcement ratio; ρ_h horizontal web-reinforcement ratio; ρ_l boundary longitudinal-reinforcement ratio; ρ_t boundary-tie reinforcement ratio; $N/A_g f_c'$ axial-load ratio; f_c' concrete compressive strength (MPa).

Table 2. Material properties of reinforcement

Bar	Straight Bars					Bent Bars			
	8 mm steel	#3 steel	#4 steel	#3 GFRP	#4 GFRP	#3 GFRP Straight portion	#3GFRP Bent portion	#3 CFRP Straight portion	#3 CFRP Bent portion
d_b (mm)	8	9.5	12.7	9.5	12.7	9.5		9.5	
A_f (mm ²)	50.3	71	129	71.3	126.7	71.3		71.3	
E_f (GPa)		200		66.9	69.6	52	---	120	---
f_{fu} (MPa)		$f_y = 400$		1412	1392	962	500	1596	1000
ε_{fu} (%)		$\varepsilon_y = 0.2$		2.11	2.00	1.85	---	1.33	---

d_b bar nominal diameter, A_f nominal cross-sectional area, E_f modulus of elasticity, f_{fu} guaranteed tensile strength, ε_{fu} ultimate strain, f_y steel yielding strength, ε_y steel yielding strain.

TEST RESULTS AND DISCUSSION

The observed damage is presented and discussed to assess the performance of FRP-RC shear walls concerning the three main structural performance levels: immediate occupancy, life safety, and collapse prevention. The limitations of the performance levels were identified based on the observation and evaluation of damage pattern for each tested wall based on the prescribed definition of damage state for each performance level according to ASCE/SEI 41 [7].

Similar hysteretic behavior was attained by the newly tested specimens ST15-R and C15 in comparison to their counterpart specimens ST15 and G15, respectively (Figure 2). The specimen ST15-R achieved higher ultimate load and drift capacities than ST15 due to its higher reinforcement ratio. The CFRP spiral stirrups confining the boundary element of the specimen C15, instead of the GFRP spiral stirrup that had been used in specimen G15, had no significant effect on the general behavior of C15 except for slight increase in the ultimate load capacity. Failure was due to concrete crushing after buckling of the longitudinal steel bars in ST15-R and was associated with longitudinal and transverse rupture of the GFRP bars and CFRP spiral stirrups, respectively, in C15.

Figure 2 shows the hysteretic response of all tested walls. In the early loading stage (immediate occupancy level), the steel-RC wall achieved a higher load than the GFRP-RC walls, due to the softened response of the GFRP-RC walls, which is an advantage of using GFRP reinforcement. The yielding plateau was evidenced in the steel-RC shear walls by the yielding of the longitudinal steel reinforcement, creating the transition point to the life safety level at 0.5% and 0.57% drift ratio for specimens ST15 and ST15-R as shown in Fig. 2a and b, respectively. The two steel-RC walls showed a stable behavior through the life safety level.

The load capacity of the FRP-RC shear walls kept increasing with increasing lateral displacement due to the linear behavior of the FRP bars. Therefore, the concrete was the source of plasticity in the FRP-RC shear walls, and the start of the life safety level could be identified based on the determination of concrete plasticity. Experimental observations of specimens G15 and C15 showed the start of concrete plasticity at 1.5% drift ratio (Fig. 2c and d), which corresponds to a concrete compressive strain $\varepsilon_c = 0.0035$. The transfer to the life safety level was evidenced by no new crack propagation, and residual forces beginning to accumulate at zero displacement. Meanwhile, during the life safety level, the FRP-RC shear walls showed recoverable and self-centering behavior, in addition to the stable behavior. Figure 2 confirms the significant difference in strength and stiffness degradation between the steel and GFRP reinforcement in the shear walls in the immediate occupancy level. The FRP-RC shear

walls recorded a significantly less stiff response after initial cracking. This is excellent behavior in resisting earthquakes, as it would increase the displacement demand which is considered as an advantage of using GFRP bars. This is due to the fact that the lower structural stiffness results in a longer natural period of vibration and, consequently, lower seismic-force demand [10].

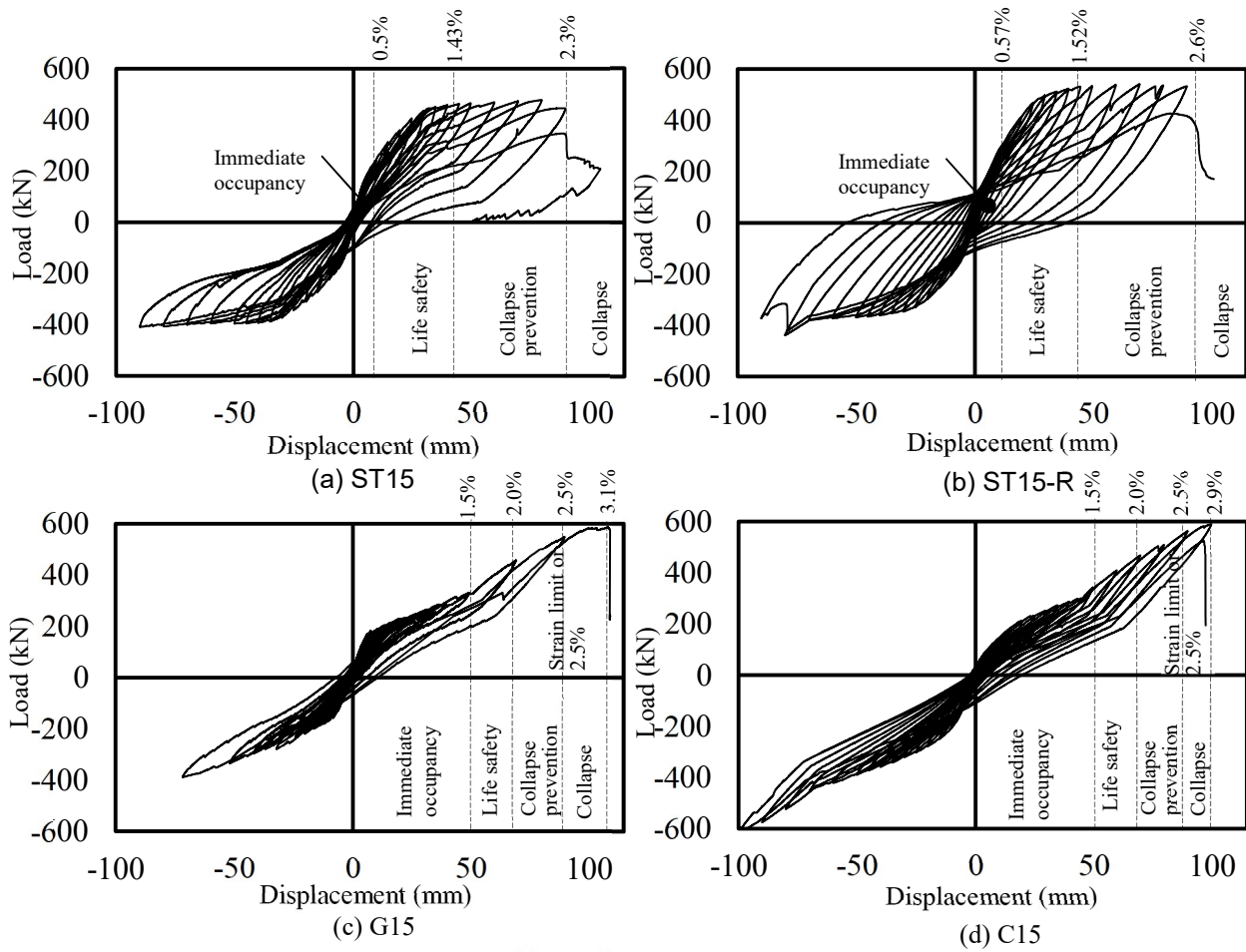


Figure 2. Hysteretic response.

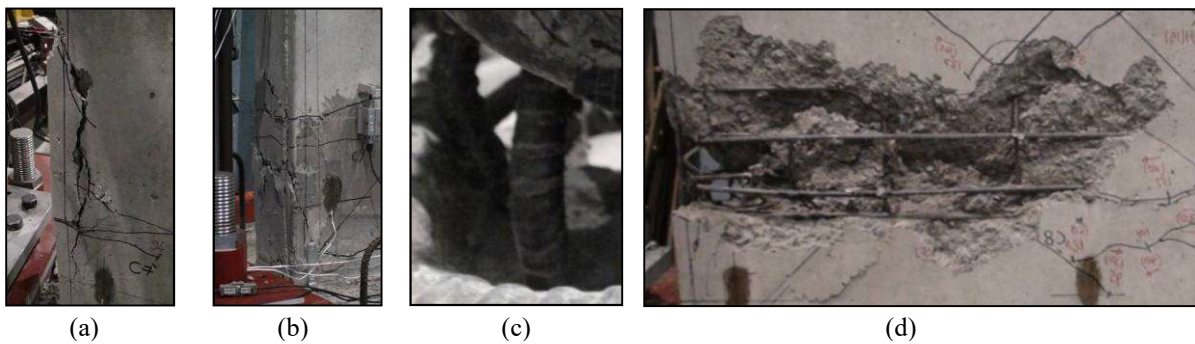


Figure 3. Failure progression of specimen ST15: (a) vertical cover splitting; (b) spalling of concrete cover; (c) buckling of longitudinal bars; and (d) concrete crushing causing failure.

Figures 3 and 4 illustrate the typical progression of flexural-shear cracking for ST15, ST15-R, G15, and C15 shear walls. For all tested walls, flexural horizontal cracks were propagated in the early loading stages, followed by diagonal cracks. In both steel-RC shear walls, the flexural cracks were propagated and were followed by yielding of longitudinal reinforcement representing the end of the immediate occupancy level. Up to the end of life safety level identified at 1.43% and 1.52% drift ratio for ST15 and ST15-R, respectively, the crack width kept increasing on the tension side of the walls, while concrete-cover splitting was observed on the compression side at the boundary zone (Fig. 3a), causing significant permanent deformation. That

formed the plastic hinge in the steel-RC shear walls and the transition to the collapse prevention level. Concrete-cover spalling and buckling of longitudinal bars in the boundary region under compression were observed (Figs. 3b and c, respectively) at around 2.0% drift ratio for the both walls (ST15 and ST15-R), at which point the steel-RC shear walls reached their ultimate capacity. In addition to the typical flexural failure, ST15 experienced major horizontal crack through the length of the wall which can be attributed to less vertical and horizontal web reinforcement ratio compared to ST15-R. Such a major horizontal crack led to an extensive concrete spalling in the compressed zone of ST15 through the plastic hinge region (Fig. 3d). Finally, specimens ST15 and ST15-R had 80% of the ultimate capacity at 2.3% and 2.6% drift ratio, respectively, defining the end of the collapse prevention level. In this level, the steel-RC shear walls experienced reduction in load capacity due to softening of tensioned steel bars and buckling of compressed steel bars (Fig. 2a and b).

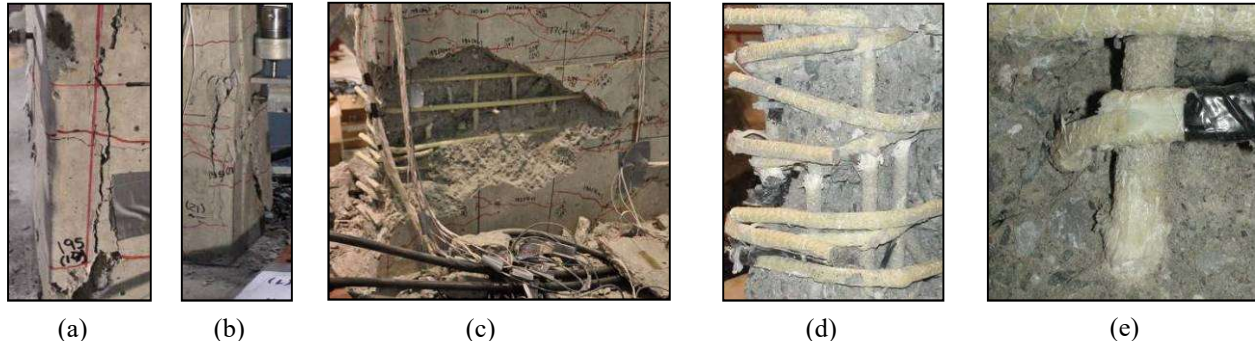


Figure 4. Failure progression of GFRP specimens: (a) vertical cover splitting; (b) spalling of concrete cover; (c) concrete crushing causing failure; (d) fracture of longitudinal bars; and (e) rupture of GFRP tie.

In the GFRP-RC shear walls, the cracks were able to close and realign after each cycle up to 1.5% drift ratio, i.e., the transition from the immediate occupancy level to the life safety level. At the end of the life safety level, the concrete cover close to the wall-base in the compressed boundary zone started to split vertically (Fig. 4a) and formed a plastic-hinge region, followed by the onset of the concrete-cover spalling at 2% drift (Fig. 4b). Although GFRP bars have a linear stress–strain behavior, Mohamed et al. (2014b) observed a plastic hinge in GFRP-RC shear walls. With increasing load, the failure of specimens G15, and C15 occurred at 3.1%, and 2.9% drift ratio, respectively. The concrete was crushed in the boundary zone under compression, associated with the fracture of longitudinal GFRP bars and rupture of GFRP and CFRP spiral stirrups (Figs. 4c, d, and e, respectively). Specimens G15, and C15 had their load-carrying capacity reduced by around 30% of their maximum capacity, proceeding to failure.

The FRP bars in the FRP-RC shear walls did not experience tension softening behavior due to their elastic nature. In addition, concrete softening under compression is ignored in comparison to the high strain that could be achieved by the FRP bars. Therefore, the FRP-RC shear walls attained high deformation capacity within the elastic strain capacity of the FRP bars, which needs to be limited to set a limit for the collapse prevention level. Accordingly, as shown in Fig. 2 c and d, the collapse prevention level in the GFRP-RC shear walls should be defined in terms of material strain limits or by setting a drift limit. The drift limit could be 2.5% to restrict non-structural damage according to Mohamed et al. [5]. Meanwhile, the strain limits could be set based on the experimental observation. The maximum recorded compressive strains were 0.0086 and 0.011 for the specimens G15 and C15, respectively, which is in the range of 0.4 to 0.5 of the ultimate tensile strain of the FRP bar. Generally, the suggested material strain limits under tension and compression could be related to the ultimate tensile strain in FRP bars; the strain could be limited in tension as $\epsilon_{frp t} = 0.9 \epsilon_{frp max}$ and, in compression, $\epsilon_{frp c} = 0.4 \epsilon_{frp max}$.

ASSESSMENT OF STRUCTURAL PERFORMANCE LEVELS

The deformation limits specified in ASCE/SEI 41 are given either in the form of drift ratio or plastic rotations, depending on the type of structural element or component under consideration. According to ASCE/SEI 41 [7], the drift ratio for the three structural performance levels of the steel-RC shear walls are 0.5% for immediate occupancy, 1% for life safety and 2% for collapse prevention levels. Figure 5 and Table 3 show comparison between the ASCE/SEI 41 [7] performance drift limits and the drift ratio experimental observation at different drift ratios corresponding to performance limits identified based on the experimental observations and associated with the damages specified in ASCE/SEI 41 [7] and ASCE/SEI 41 [9] for the tested steel- and GFRP-RC walls.

For the steel-RC shear walls, the yielding of steel reinforcement was recorded at 0.5% and 0.57% drift ratio for specimens ST15 and ST15-R, respectively, which is within the limitation of 0.5% drift ratio for immediate occupancy according to ASCE/SEI 41 [7]. For the life safety performance level, the major flexural cracking and concrete-cover splitting in addition to

the start of gaining permanent drift were observed, while the walls were still stable. These evidences were observed at 1.43%, 1.52% drift ratio for ST15 and ST15-R, respectively, which exceeded the 1% drift ratio limitation. The specimens ST15 and ST15-R had their 80% of the ultimate capacity at 2.3% and 2.6% drift ratio, respectively, identifying the collapse prevention performance level, which also exceeded the limitation of 2% (Fig. 5a). The conformity between the specified performance limits in ASCE/SEI 41 [7] and the experimental observation of ST15 and ST15-R for each performance level supports the analysis of such tested walls.

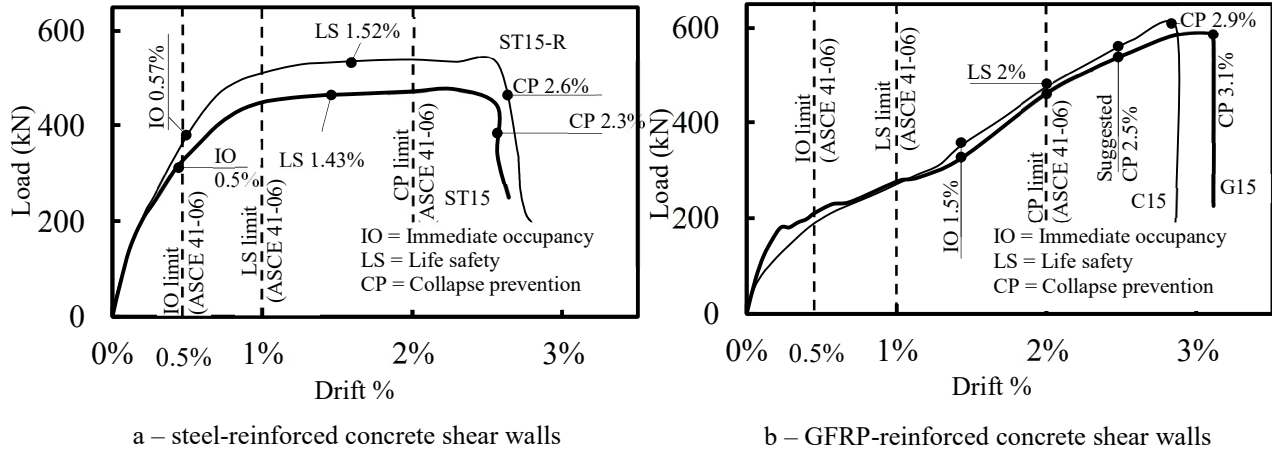


Figure 5. Assessment of structural performance levels

Table 3. Structural performance levels based on drift ratio (ASCE/SEI 41-06)

Performance levels	Level associate damage	Drift limit according to ASCE/SEI 41[7]	Drift ratio according to experimental observation			
			ST15	ST15-R	G15	C15
IO	Minor structural damage	0.5%	0.5%	0.57%	1.5%	
LS	Substantial structural damage due to inelastic material behavior. Major cracking and some spalling of concrete, but the structure remains stable with sufficient strength and deformability	1.0%	1.43%	1.52%	2%	
CP	Major flexural and shear cracks. Sliding at joints. Extensive crushing and buckling of reinforcement. Severe boundary element damage. Mark the ultimate limit prior to collapse	2.0%	2.3%	2.6%	2.5%*	
Failure	Failure of test specimens		2.3%	2.6%	3.1%	2.9%

* Collapse prevention was set to 2.5% for the GFRP-reinforced shear to restrict nonstructural damage (Mohamed et al. [5]).

For the GFRP-RC shear walls (Fig. 5b and c), the immediate occupancy performance level was identified experimentally at 1.5% drift ratio with negligible permanent deformation which clearly exceeds the immediate occupancy (0.5% drift ratio) and life safety (1% drift ratio) performance levels according to ASCE/SEI 41 [7]. This is mainly attributed to the elastic nature of the GFRP bars and the concrete is the source of plasticity (Mohamed et al. [5]). The GFRP-RC shear walls kept stable and had the ability of self-centering till a drift ratio of 2% identifying the life safety performance level which exceeds the 1% drift ratio of life safety and even reached the 2% drift ratio limit for collapse prevention level according to ASCE/SEI 41 [7]. The damage signs associated with the collapse prevention performance level; like major flexural and shear cracks and concrete cover spalling at boundary elements, were observed at 2% drift ratio, which is specified as the drift limit for the collapse prevention performance level according to ASCE/SEI 41 [7].

CONCLUSIONS

Through the presented experimental program, which consists of four tested full-scale shear walls representing one-story prototype mid-rise shear wall, the performance-based assessment of GFRP-RC shear walls was investigated. The assessment was based on comparing the drift ratio limits at immediate occupancy, life safety, and collapse prevention specified in

ASCE/SEI 41 [7] and the drift ratio obtained based on the experimental observation corresponding to the damage level associated with each of the three performance levels. The findings are promising with respect to applications for GFRP bars as follows:

- All tested steel-RC and GFRP-RC shear walls clearly comply with the ASCE/SEI 41 [7] drift ratio limitations when comparing the prescribed damage level associated with each performance level with the identified damage level based on the experimental observations. However, GFRP-RC walls overstepped these limitations.
- During immediate occupancy level, the softer response of the GFRP-RC shear walls comparing to the steel-RC shear walls is considered as an advantage of using GFRP bars as it would increase the displacement demand and attracting lower seismic force demand.
- Due to the elastic nature of the GFRP bars and to prevent the brittle failure, setting the collapse prevention at 2.5% is recommended to restrict non-structural damage.
- The GFRP bar strain could be limited at the collapse prevention level in tension and compression to 90% and 40% of the ultimate tensile strain of GFRP bar.
- Limiting the GFRP-RC walls' drift ratio according to ASCE/SEI 41 [7] at the immediate occupancy and life safety levels is not representative as the walls still experience self-centering behavior with negligible permanent deformation with low damage levels.

ACKNOWLEDGEMENTS

The authors wish to acknowledge the financial support of the Natural Sciences and Engineering Research Council of Canada (NSERC), the Canada Research Chair in Advanced Composite Materials for Civil Engineering, and the Fonds québécois de la recherche – Nature et Technologies - (FQRNT) of Quebec.

REFERENCES

- [1] Fintel, M., 1991. "Shear walls—An answer for seismic resistance?" *Concrete International*, 13(7), 48–53.
- [2] ACI Committee 318, "Building Code Requirements for Structural Concrete and Commentary (ACI 318-14)," American Concrete Institute, Farmington Hills, MI, 2014, 503 pp.
- [3] Canadian Standards Association A23.3, "Design of concrete structures standard (CSA A23.3-14)," Mississauga, ON, Canada, 2014, 240 pp.
- [4] Mohamed, N., Farghaly, A. S., Benmokrane, B., and Neale, K.W., 2014a. "Experimental investigation of concrete shear walls reinforced with glass fiber–reinforced bars under lateral cyclic loading." *Journal of Composites for Construction*, ASCE, 18(2), A4014001.
- [5] Mohamed, N., Farghaly, A. S., Benmokrane, B., and Neale, K.W., 2014b. "Drift Capacity Design of Shear Walls Reinforced with Glass Fiber-Reinforced Polymer Bars." *ACI Structural Journal*, 111(6), 1397-1406.
- [6] Mohamed, N., Farghaly, A. S., Benmokrane, B., 2015. "Aspects of Deformability of Concrete Shear Walls Reinforced with Glass Fiber–Reinforced Bars." *Journal of Composites for Construction*, ASCE, 19(5), 06014001.
- [7] ASCE/SEI 41, "Seismic rehabilitation of existing buildings (ASCE/SEI 41-06)." American Society of Civil Engineering (Structural Engineering Institute), Reston, VA, 2006, 427 pp.
- [8] Park, R., 1989. "Evaluation of ductility of structures and structural assemblages from laboratory testing." *Bull. N. Z. Nat. Soc. Earthquake Eng.*, 2(3), 155-166.
- [9] ASCE/SEI 41, "Seismic Evaluation and Retrofit of Existing Building (ASCE/SEI 41-13)." American Society of Civil Engineering (Structural Engineering Institute), Reston, VA, 2013, 555 pp.
- [10] Sharbatdar, M. K., and Saatcioglu, M., 2009. "Seismic Design of FRP Reinforced Concrete Structures." *Asian Journal of Applied Sciences*, 2(3), 211-222.